

An experimental study of the dynamic characteristics of the catenary-pantograph interface in high speed trains

Jung Soo Kim*

*Department of Mechanical and System Design Engineering, College of Engineering, Hongik University
72-1 Sangsu-dong, Mapo-gu, Seoul 121-791, Korea*

(Manuscript Received June 11, 2007; Revised July 5, 2007; Accepted July 6, 2007)

Abstract

The dynamic characteristics of the catenary-pantograph interface in high-speed trains are evaluated. During a test run signals from accelerometers, load cells, and strain gauges attached to various parts of the pantograph assembly are collected and processed. The signals are analyzed in both the time and frequency domains to determine the dynamic characteristics of the catenary-pantograph interface constituting the critical part of the current collection system of the high-speed train. It is found that there are major frequency components of the pantograph motion at the interface that shift in direct proportion to the train speed as well as components that are stationary in the frequency domain such as the 8.5 Hz component representing the fundamental resonant mode of the panhead assembly. The contact force at the interface shows that while the mean contact force stays almost invariant, the fluctuating component is significantly dependent on the filtering frequency applied to the accelerometer signal during estimation of the inertia force of the panhead. An important implication of the finding is that analytical or numerical investigations based on lumped element models of the pantograph may provide accurate predictions on mean values of the contact force at the catenary-pantograph interface, but are inherently limited in estimating high-frequency fluctuations in the contact force. Since the ratio of the fluctuating portion to the steady-state portion (i.e., the mean value) increases with increased train speed, the predictive capacity of the investigations based on numerical simulations diminishes with increasing train speed.

Keywords: Catenary; Contact force; Current collection system; Dynamics; High speed train; Pantograph

1. Introduction

The current collection system in high-speed trains provides the required electrical power to the train. Two major elements of this system are the catenary and the pantograph. The catenary is an overhead slender structure composed of wires, repeating spans, and hangers. The pantograph is a device that acts as a conduit for delivering electrical power from the catenary to the train. During train operation, the pantograph and catenary must remain in physical contact at all times since the separation causes power loss and high temperature arcs forming at the interface be-

tween them. As the magnitude of the dynamic fluctuations tends to increase with increased train speed, ensuring proper contact at the catenary-pantograph interface has become a critical issue for high-speed trains. Therefore, proper understanding of the dynamic properties of the catenary-pantograph interface is essential to ensure reliable train performance.

The catenary-pantograph system is a fairly complex system and several approaches have been taken to investigate the dynamics of the catenary and pantograph at the interface between them. Perhaps the most popular approach due to its ease and economy is the mathematical modeling and analysis of the catenary-pantograph dynamics. Choi and Chung [1], Park et al. [2] performed numerical analyses of the catenary-pantograph motion based on finite difference

*Corresponding author. Tel.: +82 2 320 1471, Fax.: +82 2 322 7003
E-mail address: jungsoo@hongik.ac.kr

schemes, while Arnold and Simeon [3] investigated mathematical properties of a numerical solution of the interaction between the catenary and pantograph. Some studies have focused on the dynamical properties of the catenary alone. The wave propagation characteristics of a simplified catenary structure with idealized boundary conditions have been investigated by Kim et al. [4]. By constructing a more detailed finite element model, Kim et al. [5, 6] investigated the modal and dynamic properties of the catenary as the design parameters are varied. Another line of investigation has been the characterization of the dynamics of the pantograph. Seering et al. [7] constructed a nonlinear, lumped parameter model and compared the model predictions with experimental data. Park et al. [8] performed a dynamic sensitivity analysis of a lumped parameter model of the prototype pantograph for high-speed train based on a new concept design involving reduced panhead mass [9].

On the experiment side, various investigations have utilized dynamically scaled-models. For instance, Farr et al. [10], Willets and Edwards [11] constructed dynamically equivalent laboratory scale models to study the effect of the design variables on the behavior of the catenary-pantograph interface for low speed trains. Owing to scaling factors as high as 40:1, significant distortions were perhaps inevitable in their results. Delfosse and Sauvestre [12] sought to improve the reliability of the measurement procedure for determining the vertical motion of the catenary. By designing and constructing a scaled model for high-speed trains, Manabe [13] found that the performance of the catenary-pantograph system rapidly deteriorates with increasing train speed. He found the wave propagation velocity of the catenary to be a critical factor in determining the interface dynamics.

Owing to great difficulty of planning and implementing full-scale measurement as well as the difficulty of making modifications on the catenary-pantograph system for attaching appropriate sensors, relatively few investigations based on full-scale test runs have been reported. And the few that have been reported tended to be limited verifications of the overall system performance and not an in-depth analysis of the catenary-pantograph interface dynamics. [14] In the present study, the dynamic characteristics of the catenary-pantograph interface at full-scale are investigated based on signals acquired during an actual test run of a high-speed train. The present work builds on recent work by the author in which the ef-

fect of the motion of the train on the interface dynamics has been explored [15].

The organization of the paper is as follows. In section 2, the signals collected at the catenary-pantograph interface are presented in the time domain, while in section 3 the same signals are analyzed in the frequency domain. Section 4 presents experimental findings on the characteristics of the contact force at the interface of the catenary and the pantograph. Finally, the results are summarized in section 5.

2. Interface dynamics in the time domain

The overall structure of the catenary-pantograph system is shown in Fig. 1. In the catenary, the electrical current is actually supplied to the train through the contact wire connected to the messenger wire by hangers. The hangers serve to transmit the weight of the contact wire onto the messenger wire. The span posts are used to provide vertical support for the catenary structure. There are devices called steady arms for providing lateral adjustment needed to protect the panhead from localized wear by moving the catenary sideways. Each span and hanger is given a predetermined sag, and as will be described later, the span spacing and the hanger spacing serve as important sources of vibratory motion of the pantograph. The pantograph is composed of three main segments and suspensions connecting them. The segment that comes in actual contact with the catenary (i.e., contact wire) is called the panhead.

Fig. 2 shows the speed profile of the test run from which the signals are acquired and analyzed. The maximum speed in the present test run is 200 km/hr, equivalent to 55.5 m/s. It can be surmised that the pantograph will be exposed to harsher conditions as the speed of the train increases due to increased train motion and air resistance. We will therefore focus our attention on the analysis of signals at or near 200 km/hr.

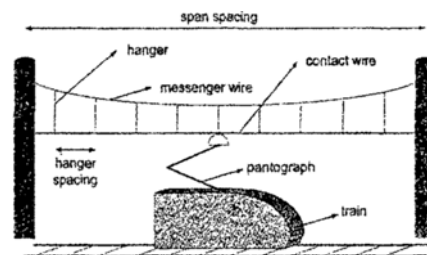


Fig. 1. Catenary-pantograph system.

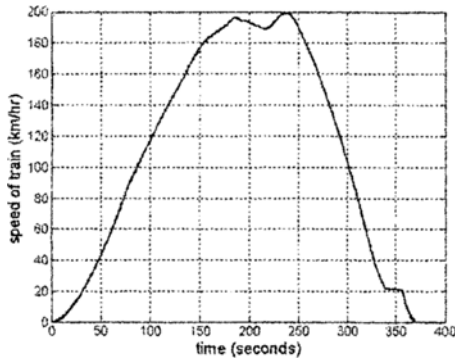


Fig. 2. Speed profile of test run.

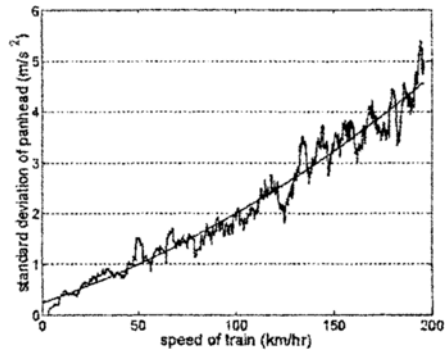


Fig. 5. RMS acceleration vs. train speed.

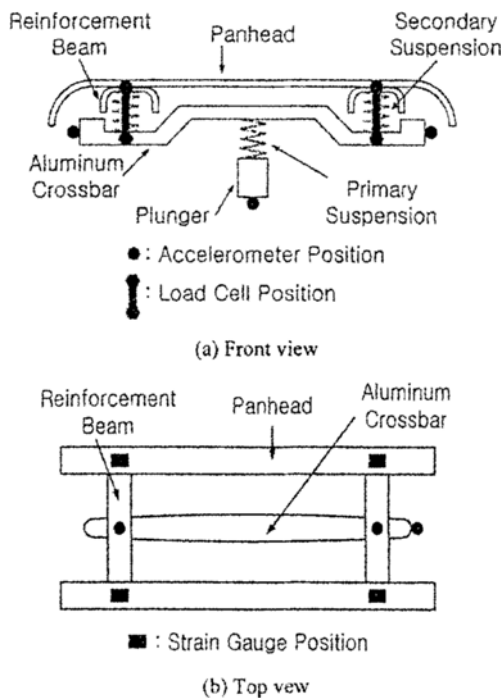


Fig. 3. Sensor locations.

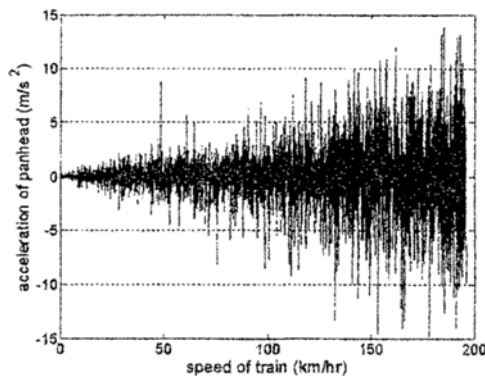


Fig. 4. Panhead acceleration vs. train speed.

Figs. 3 (a) and 3 (b) describe the positions of the sensors attached to the pantograph assembly during the test run. To measure the movement of the panhead that comes in contact with the contact wire of the catenary, two accelerometers are attached on top of the reinforcement beams that connect the front and rear panheads. Although it would be desirable to place the accelerometers on the panhead itself, it is not possible since the sensors will interfere with the current collection taking place between the contact wire and the panhead. Therefore, the accelerometers are placed on the reinforcement beams which are the next suitable position and will herein be referred to as the panhead acceleration. Also, two load cells are placed between the panhead and aluminum crossbar below.

Figs. 4 and 5 show the panhead (actually the left reinforcement beam) acceleration level and its root mean square (RMS) level as functions of the train speed, respectively. The rate of the increase in the acceleration is found to be roughly proportional to the square of the train speed. Thus, the catenary-pantograph interface is subject to more vibration as the train gains speed.

Fig. 6 depicts the load on suspensions as a function of the train speed. The sinusoidal profile evident in a single load cell signal is due to the stagger of the catenary effected through the action of the steady arm. The stagger moves the point of contact left and right, delocalizing the point of contact and evenly spreading wear on the panhead. The load cell (located at a certain distance away from the center of the panhead) reaches a local maximum when the point of contact staggers closest to it and a local minimum when the point staggers farthest from it. The period of a cycle is observed to diminish as the train speed increases because it is inversely proportional to the train speed.

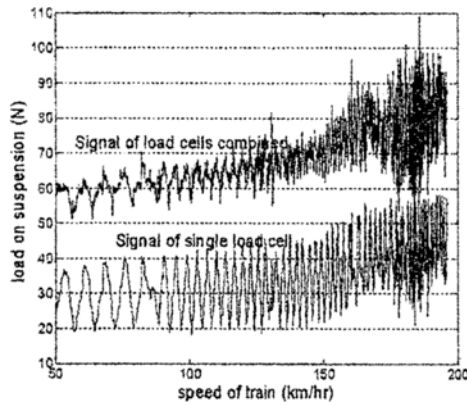


Fig. 6. Load vs. train speed.

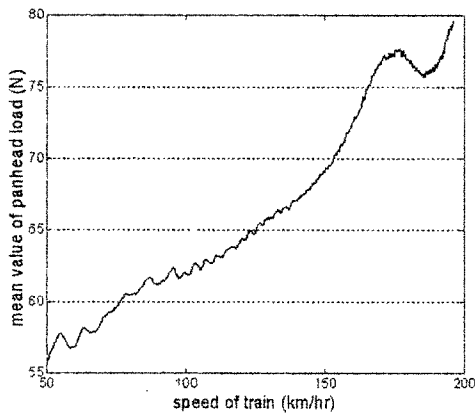


Fig. 7. Mean value of combined load.

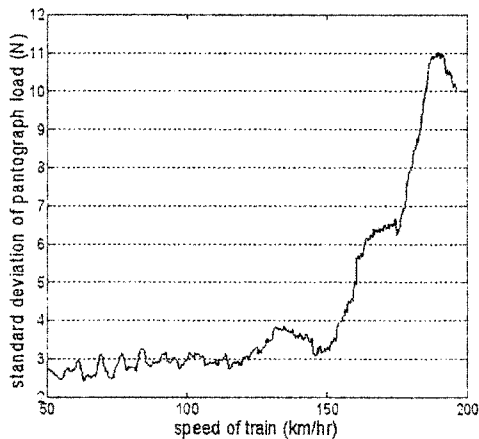


Fig. 8. Fluctuation in combined load.

The period of this sinusoid corresponds to the time required for the train to traverse a span. The inverse of the period is the span-passing frequency. Figs. 7 and 8 show the mean and the standard deviation of the combined load, respectively.

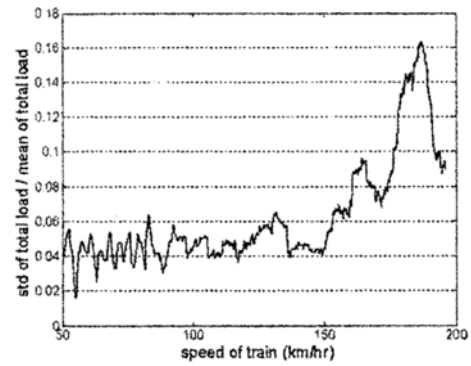


Fig. 9. Variation / mean.

Fig. 9 shows the standard deviation of the load divided by the mean of the same load. This ratio remains low until 150 km/hr then rapidly increases. The increase in this ratio refers to relatively greater fluctuating components of the contact load, which is not desirable from the stable interface dynamics point of view.

3. Interface dynamics in the frequency domain

Figs. 10 (a) and 10 (b) show the left reinforcement beam accelerometer signal at the train speed of 196 km/hr in the frequency domain. Several major frequency components can be observed in Fig. 10 (a). The first peak at 1.4 Hz is the span-passing frequency. The train speed is 196 km/hr and from the load cell data, the length of the span is measured to be 40 m. The time elapsed for the train to traverse the span length is 0.73 seconds. Taking the inverse, the frequency is found to be 1.4 Hz. The higher harmonics of the span-passing frequency are also observed. These harmonics have a frequency of twice and three times the span-passing frequency and appear intermittently throughout the run. Since this component arises from the interaction between the pantograph and the catenary as the pantograph traverses along the prescribed sag in the contact wire, it is dependent on the train speed. The span-passing frequency shifts in direct proportion to the increase in the train speed.

The hanger-passing frequency component, i.e., the frequency corresponding to the train traversing the hanger length which is 1/9 of the span length - there are nine hangers per span - is also speed dependent. However, this component is not pronounced in the measurement. This finding does not correlate well with the simulated response of Kim et al. [6] that has predicted the hanger-passing component be signifi-

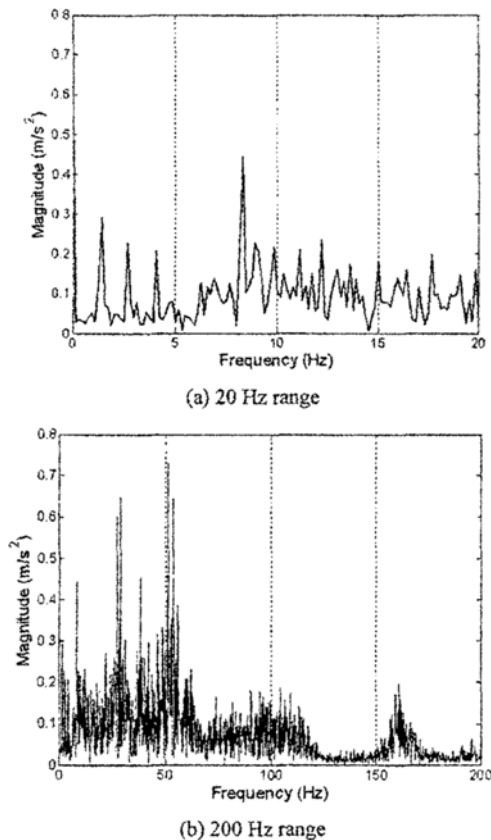


Fig. 10. Frequency components of panhead motion.

cant. A part of the reason for the apparent discrepancy is that the hanger-passing frequency components may overlap with the other resonant modes.

A large peak observed at 8.5 Hz is due to the fundamental resonant mode of the panhead assembly. Unlike the span-passing frequency component, this component is independent of the train speed. Previously reported numerical simulation results corroborate this observation: A simulation run based on finite difference modeling of the identical catenary and pantograph has predicted that the resonant mode at 8.5 Hz will be an important part of the pantograph motion [2].

Higher frequency components due to the structural vibration of the pantograph are illustrated in Fig. 10 (b) by enlarging the window in the frequency domain. Although due discretion is needed since the accelerometers are attached to the reinforcement beams rather than directly to the panhead, it has been independently verified that the measured signal contains major vibration components of the panhead structure: The 28 Hz and the 160 Hz component are the 1st

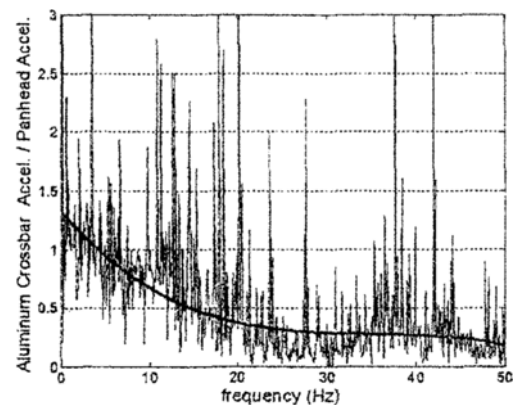


Fig. 11. Transfer function (Al X-bar / panhead).

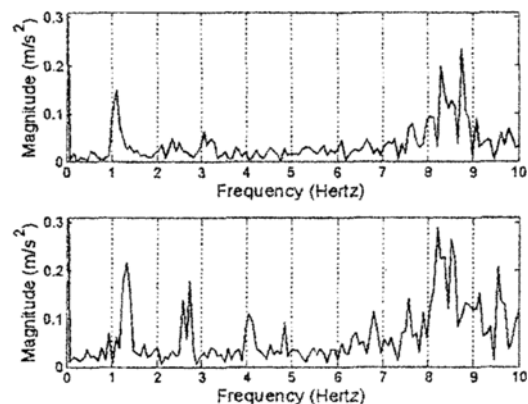


Fig. 12. Shifts in span-passing frequency.

bending frequencies of the reinforcement beam and the panhead itself, respectively. The 52 Hz component could not be fully characterized at this moment, but is believed to be related to the structural vibration of the panhead assembly.

Fig. 11 shows the transfer function between the accelerations of the aluminum cross bar and the panhead. Disregarding the spikes due to the structural and joint vibrations, the overall ratio drops below 0.5 at 20 Hz. This suggests that the suspension installed between the panhead assembly and the aluminum cross bars works as a vibration isolator, as it is designed to be [9].

To illustrate the speed-dependent nature of the acceleration signal, Fig. 12 compares the frequency components of the panhead at two different train speeds. The speed for the upper graph is 147.6 km/hr and the lower is 193.29 km/hr. Since the train speeds of the two graphs differ, the speed dependent span-passing component must also differ by the same

amount. The first peak for the upper graph is placed at 1.09 Hz and the lower graph is at 1.33 Hz. The first peak shifts to a higher frequency as the train speed increases. As expected, this shift in the first peak occurs continuously as the train speed varies throughout the test run. It can also be seen that the frequency of the speed-independent 8.5 Hz component remains stationary irrespective of the train speed.

Fig. 13 compares the frequency response of the

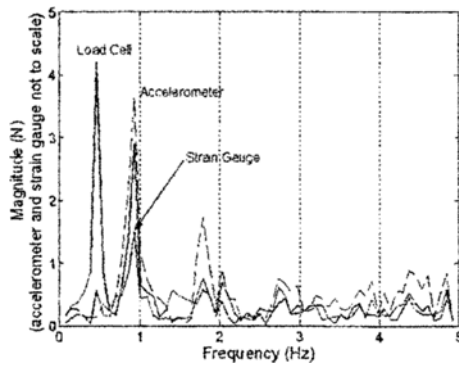


Fig. 13. Frequency components of sensors.

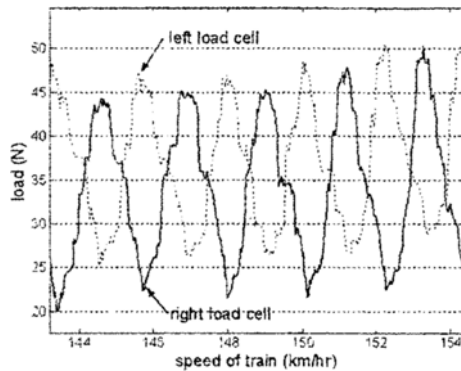


Fig. 14. Rolling motion of panhead.

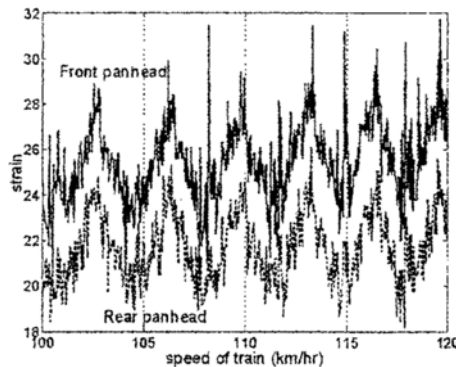


Fig. 15. Pitching motion of panhead.

load cell together with the accelerometer and strain gauge signals. The first peak of the accelerometer signal coincides with the second peak of the load cell signal and the first peak of the strain gauge signal, and represents the span-passing component.

The first peak observed in the load cell signal is one-half of the span-passing frequency and is a result of the rolling motion caused by the stagger induced in the catenary by the steady arms. The load cell must traverse two spans to complete a rolling motion. The presence of the rolling motion is further demonstrated by the opposite phases of the left and right load cells. (Fig. 14) Although a rolling motion exists, an undesirable pitching motion that may adversely affect the interface dynamics does not occur: the front and rear panheads are in phase as shown by the strain gauge signals attached underneath the front and rear panheads. (Fig. 15) The absence is due to the perfect symmetry of the pantograph design in the front-rear direction.

4. Contact force determination

The contact force existing between the catenary and the panhead is an important indicator of the performance of the current collection system. It determines both the separation ratio of the current collection system and the wear rate of the catenary and the panhead. If the contact force is too low, increased separation rate will result in excessive arcs and lead to the erosion of localized areas of the panhead. On the other hand, if the contact force is too high, the panhead will maintain contact with the catenary but at the cost of increased wear of the panhead. Therefore, the contact force needs to be maintained within a specified range.

A direct measurement of the contact force would require sensors to be placed at the interface between the contact wire and the panhead. However, this is not feasible due to a relative motion as well as high voltage current passing between them. A preferred method for getting around this problem is to place the load cells below the panhead. But by doing so, the inertia force due to the movement of the panhead must be considered, i.e., the measured load cell signals need to be compensated by properly accounting for the acceleration of the panhead mass. The contact force can be represented as a sum of the load measured by the load cells attached to the bottom of the panhead, and the inertia force due to the panhead

acceleration.

$$F_{\text{contact}} = F_{\text{load cell}} + F_{\text{panhead inertia}} \quad (1)$$

The methodology for calculating the inertia force from the accelerometer signals is now addressed. In our calculation of the inertia force, we will for now assume rigid body acceleration of the panhead which enables us to ignore, i.e., to filter out high frequency components of the accelerometer signal originating from the structural vibration of the panhead. Since the 8.5 Hz component represents the major resonant mode of the panhead assembly in which the overall panhead motion takes place over the suspension, i.e., since it is the major frequency component and it is below the structural vibration frequencies, a 12 Hz low-pass filtering is probably adequate to ensure that all structural vibration components are filtered out. With the rigid body assumption, the inertia force can be computed as a simple product of the panhead acceleration and the panhead mass. Equation (1) takes on a simple form given by

$$F_{\text{contact}} = F_{\text{load cell}} + m_{\text{panhead}} \cdot a_{\text{accelerometer}} \quad (2)$$

This approach is in line with most of the analytical and numerical studies that are based on lumped parameter models of the pantograph in which the panhead is treated as a lumped mass element. [1, 2, 7-9] The calculated contact force using Eq. (2) with a 12 Hz low-pass filtering applied to the panhead accelerometer signal is shown in Fig. 16(a).

The panhead is actually a beam rather than a rigid body, however, and the inertia force contribution of the structural vibration of the panhead cannot be neglected if greater accuracy is desired. We now investigate the effect of including higher frequency components in the accelerometer signal in the inertia force estimation. Figs. 16(b) and 16(c) show the calculated contact force with low-pass filtering at the cutoff frequencies of 20 Hz and 30 Hz, respectively. By increasing the cutoff frequency, the rigid body restriction is removed as more and more structural vibration components within the panhead motion come into play.

Strictly speaking, the calculation of the panhead inertia force as a simple product of the panhead mass and the accelerometer signal with a 20 Hz or a 30 Hz filtering applied to it is at best a rough estimate. The structural vibration of the panhead involves a relative

motion between different locations within the panhead, and the many more acceleration measurements at selected locations within the panhead structure are probably needed to accurately determine the structural vibration contribution to the panhead inertia force. As a practical matter, the inertia force can be calculated as a weighted sum of all the accelerometer signals collected at selected locations within the panhead, with the weighting factor for each signal suitably determined. For greater accuracy, a greater number of such acceleration signals with suitably determined weighting factors will be required. In the present study, just two accelerometer signals are used with an equal weighting factor of 1/2 for each. Equation (2) is still applicable but with the panhead acceleration term expanded to include the higher frequency contributions due to the structural vibration. The contact force calculated according to equation (2) is expected to provide a satisfactory qualitative trend, if not accurate quantitative predictions.

Fig. 17 divides the predicted contact forces into the mean and fluctuating parts for different cutoff frequencies. The mean value of the predicted contact force increases with the train speed, but the influence of the cutoff frequency on the mean is found to be insignificant. In contrast, the fluctuation of the contact force from the mean as measured by the standard deviation is significantly affected by the cutoff frequency as shown at the bottom of Fig. 17. At the top train speed of 200 km/hr, the mean contact force is found to be around 85 N for all three cutoff frequencies, while almost two-fold increase in the standard deviation from 11 N to 20 N is observed between the 12 Hz and 30 Hz cutoff frequency. For comparison, Kim et al. [5] with a 20 Hz low-pass filtering applied to the simulation output have reported a mean contact force of 121.5 N with the standard deviation of 14.7 N.

An important implication of the present finding is that analytical or numerical investigations based on multi-degree-of-freedom discretized models of the catenary and/or pantograph could provide accurate predictions of the mean value of the contact force but may not fully account for fluctuations dominated by the high-frequency structural vibration components. Since the ratio of the fluctuating portion to the mean value portion in the contact force increases with increasing train speed, the predictive capacity of the investigations based on numerical simulations utilizing lumped parameter models of the pantograph di-

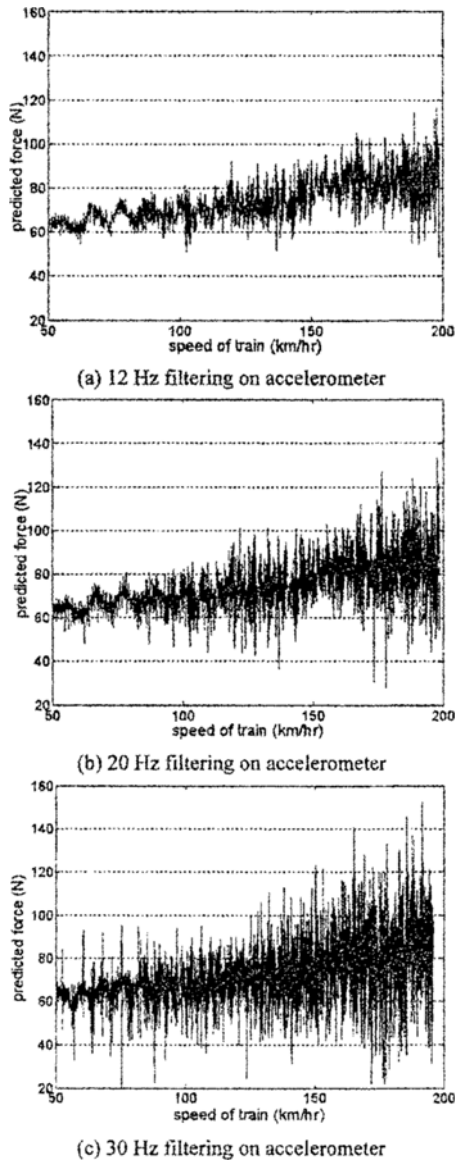


Fig. 16. Contact force vs. train speed.

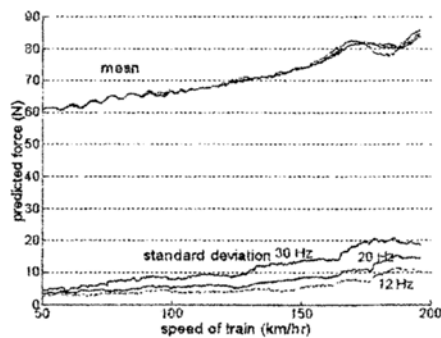


Fig. 17. Mean and fluctuation of contact force.

minishes with increased train speed.

5. Conclusions

The dynamic characteristics of the catenary-pantograph interface in high-speed trains are evaluated by examining signals collected from various sensors during a test run. The overall acceleration of the pantograph at the interface increases to the square of the train speed. The measured panhead motion shows the presence of a rolling mode, but an undesirable pitching mode is absent due to the symmetry of the pantograph design.

The frequency domain analysis of the accelerometers and the load cells has isolated major frequency components of the catenary-pantograph interface dynamics such as the span-passing, hanger-passing, and the fundamental resonant mode of the panhead assembly, as well as a number of structural bending vibration modes. They can be divided into components that shift in direct proportion to the train speed, such as the span-passing modes and into stationary components such as the 8.5 Hz panhead assembly resonant mode and a multitude of structural vibration modes.

The contact force can be calculated by taking a sum of the load cell signals and the panhead inertia force. The inertia force calculation uses the accelerometer signal low-pass filtered with a suitable cutoff frequency. The mean value of the contact force does not vary much as the cutoff frequency is varied, but the fluctuation about the mean increases as the cutoff frequency is increased to allow structural vibration components. Thus, the choice of a cutoff frequency will significantly influence the predicted fluctuation about the mean but not the mean value of the contact force.

An important implication of the present finding is that the analytical and numerical investigations based on multi-degree-of-freedom discretized models of the catenary and/or pantograph may provide accurate predictions on the mean values of the contact force at the catenary-pantograph interface but are inherently limited in describing fluctuations about the mean. Since the ratio of the fluctuating portion to the steady-state portion (i.e., the mean value) increases with increased train speed, the predictive capacity of the investigations based on numerical simulations tend to diminish with increasing train speed.

Acknowledgment

The author is grateful for the support provided by a grant from Seoul City New Technology R&D Business Program.

References

- [1] Y. S. Choi and D. H. Joung, Numerical analysis of dynamic response of catenary/pantograph system in high-speed train, *SKKU J. of Science and Technology* 42(2) (1991) 377-390.
- [2] S. H. Park, J. S. Kim, S. Hur, J. H. Kyung and D. H. Song, On dynamic characteristics of TGV-K pantograph-catenary system, *Proc. KSR* (1999) 176-184.
- [3] M. Arnold and B. Simeon, Pantograph and catenary dynamics: a benchmark problem and its numerical solutions, *Applied Numerical Mathematics* 34 (2000) 345-352.
- [4] Y. H. Kim, Y. K. Park, S. M. Kim and H. S. Roh, Wave propagation characteristics along a catenary and arbitrary boundary conditions, *Trans. KSME* 16(11) (1992) 2059-2071.
- [5] J. S. Kim and S. H. Park, Dynamic simulation of KTX catenary system for changing design parameter, *J. KSNVE* 11(2) (2001) 346-353.
- [6] W. M. Kim, J. T. Kim, J. S. Kim and J. W. Lee, A numerical study on dynamic characteristics of a catenary, *KSME Int. J.* 17(6) (2003) 860-869.
- [7] W. Seering, K. Armbruster, C. Vesely and D. Wormley, Experimental and analytical study of pantograph dynamics, *J. Dynamic Systems, Measurement and Control* 113 (1991) 242-247.
- [8] T. J. Park, C. S. Han and J. H. Jang, Dynamic sensitivity analysis for the pantograph of a high-speed rail vehicle, *J. Sound and Vibration* 266 (2003) 235-260.
- [9] H. S. Han, J. H. Kyung, D. H. Song and J. C. Bae, Concept design of the pantograph for high speed trains, *Proc. KSR* (1998) 337-344.
- [10] D. S. Farr, H. C. Hall and A. L. William, A dynamic model for studying the behaviour of the overhead equipment used in electric railway traction, *Proc. IEE* No. 3530U (1961) 421-434.
- [11] T. A. Willetts and D. R. Edwards, Dynamic-model studies of overhead equipment for electric railway traction, *Proc. IEE.* 133(4) (1966) 690-696.
- [12] P. Delfosse and B. Sauvestre, Measurement of contact pressure between pantograph and catenary, *French Railway Review* 1(6) (1983) 497-505.
- [13] Manabe, K. High speed contact performance of a catenary-pantograph system, *JSME Int. J.* 32(2) (1989) 200-205.
- [14] S. I. Seo, C. S. Park, Y. H. Cho, K. Y. Choi, J. Y. Mok and B. B. Kang, Test and evaluation of the pantograph for Korean high speed train, *KRRI Report* (2003).
- [15] J. S. Kim, The effect of train motion on dynamic characteristics of current collection system, *J. KSR* 9(1) (2006) 18-22.